Chemical Physics 115 (1987) 243–252
North-Holland, Amsterdam

ELECTRONIC AUTOIONIZATION IN CARBON MONOXIDE: THE EFFECTS OF THE VIBRATIONAL MOTION

B. LEYH [a,b,1], J. DELWICHE [a,b,2], M.-J. HUBIN-FRANSKIN [a,b,2] and I. NENNER [a,c]

[a] *Laboratoire pour l'Utilisation du Rayonnement Electromagnétique, Laboratoire mixte CNRS, CEA et MEN, Université de Paris-Sud, bâtiment 209 D, 91405 Orsay Cedex, France*
[b] *Département de Chimie générale, Université de Liège, 4000 Sart-Tilman par Liège 1, Belgium*
[c] *CEA, IRDI/DESICP Département de Physico-chimie, Centre d'Etudes Nucléaires de Saclay, 91191 Gif-sur-Yvette Cedex, France*

Received 6 February 1987

New continuous measurements of the vibrationally resolved photoionization cross sections of CO^+ $X\,^2\Sigma^+$ and $A\,^2\Pi$ between 63 and 83 nm are reported. We assign the Rydberg series converging to CO^+ $A\,^2\Pi$. The effects of the vibrational motion are interpreted on the basis of the Condon approximation. This approximation is shown to allow a qualitative understanding of the decay of the Rydberg series converging to the $A\,^2\Pi$ and $B\,^2\Sigma^+$ states of CO^+.

1. Introduction

At low photoelectron kinetic energy, molecular photoionization is markedly influenced by the existence of resonances which trap for a more or less long time the escaping electron in the region of the ionic core (internal region) [1,2]. Two types of resonances must be distinguished [1]: the shape resonances which have a very short lifetime (about 10^{-16} s) and are therefore broad (typically a few eV), and the autoionizing resonances which are in most cases long-lived, at the atomic time scale (about 10^{-14} s), and thus relatively narrow. This latter behaviour results from the fact that the decay of the autoionizing resonances involves an energy transfer between the ionic core and the excited electron. An important example concerns the Rydberg states converging to an excited electronic ionic state, which autoionize electronically in the continuum of a low-lying electronic ionic state.

Apart from a modulation of the total photoionization cross section, these Rydberg states lead also to strong variations of the branching ratios (electronic and vibrational) between the open channels. An important problem is the behaviour of the vibrational branching ratios, i.e. the probability of producing different vibrational levels of a given electronic ionic state, along the Rydberg resonances.

In the absence of any resonance, the production of a given vibrational state is generally well accounted for by the Condon approximation associated to the direct ionization process. This approximation neglects the variation of the electronic transition moment with the internuclear distance. The vibronic transition moment is then written as a simple product of the electronic transition moment and of the overlap integral between the vibrational functions. In this case, the vibrational branching ratios are given by the Franck–Condon factors between the initial neutral state and the considered vibrational level of the ion.

If a Rydberg autoionizing resonance is present, one generally observes a modification of the vibrational excitation in the photoelectron spectra. Ex-

[1] "Aspirant" du Fonds National de la Recherche Scientifique de Belgique.
[2] "Chercheur qualifié" du Fonds National de la Recherche Scientifique de Belgique.

amples have been evidenced in CO [3–5], N_2 [4], NO [6], O_2 [4,7] and CO_2 [8–10]. In this case, we must consider simultaneously three possible transitions: the transitions to the ionization continuum and to the Rydberg state, characterized by their respective transition moments and the transition between these two states, described by its interstate coupling. We can, in a first approximation, assume that the electronic quantities associated with these transitions (transition moments and interstate coupling) do not vary with R: this is still the Condon approximation. In this framework, the vibrational branching ratios will no more depend on a single vibrational overlap but on three overlaps corresponding to the abovementioned interactions. The on-resonance branching ratios will therefore be very different from their off-resonance values leading possibly to extensions of the vibrational structure of the photoelectron bands.

This situation can be more or less deeply altered if the Condon approximation is not valid. The most striking consequence of the breakdown of this approximation is the possibility of accounting for the pure vibrational autoionization: a discrete and a continuum state, corresponding to the same electronic ionic core, which are not coupled within the Condon approximation, can now interact, giving rise to the so-called pure vibrational autoionization.

An interesting question, arising when one analyses experimental spectra is then the following: Do the observed vibrational branching ratios along the resonances actually result from a breakdown of the Condon approximation or, on the contrary, is it possible to account for the experimental results without giving up this simplifying assumption?

In general, answering this question is not at all straightforward; the use of a model based on the Condon approximation can help clarifying the problem.

To check whether the simple model based on the Condon approximation is valid in an actual case, we report here continuous measurements of the vibrationally resolved cross sections corresponding to the $X\ ^2\Sigma^+$ and $A\ ^2\Pi$ ionic states in the 63–83 nm region (19.7–14.9 eV). Electronic autoionization is indeed known to be important in this region [5,11–17] and perturbations in the vibrational distributions have already been observed at a few isolated wavelengths [3–5] and in particular, at those of the NeI resonance lines [3]. Apart from the study of the decay of these resonances, another aim of our work is to elucidate the assignments of the Rydberg series converging to CO^+ $A\ ^2\Pi$ for which no detailed analysis has been given up to now: this will complete our previous work on the Rydberg series converging to the $B\ ^2\Sigma^+$ state of CO^+ [18].

The spectral range above 75 nm ($h\nu < 16.53$ eV) is dominated by the Rydberg series converging to CO^+ $A\ ^2\Pi$ (R_A series). As a result of the important difference of equilibrium geometry between CO $X\ ^1\Sigma^+$ ($R_e = 1.128$ Å [19]) and CO^+ $A\ ^2\Pi$ ($R_e = 1.244$ Å [19]), vibrational progressions up to $v = 9$ are observed [4]. The progressions observed by Henning [11] [H(1) and H(2)], Tanaka [12] [P(1), P(2) and P(3) progressions and α series], Huffmann et al. [13] have been classified by Ogawa and Ogawa [15] in five series of several progressions. These authors [15] report the energies corresponding to the most intense series (called R_A-I).

At higher energy, the Rydberg series converging to $B\ ^2\Sigma^+$ (R_B series) also perturb the photoionization spectra. The four major series observed in this region [12–16] (called "sharp", "diffuse", III and IV) have been recently assigned by Leyh and Raşeev [18]. Between 17 and 17.5 eV, the first members of the Rydberg series converging to $B\ ^2\Sigma^+$ interact with the $n > 10$ members of the R_A series giving rise to complicated structures [15,20]. We must also mention a strong discrepancy between the results obtained by fluorescence excitation spectroscopy [21] and by photoelectron spectroscopy [22,23] about the decay of the R_B series in the $A\ ^2\Pi$ and $X\ ^2\Sigma^+$ continua.

This paper is organized as follows: in section 2, we recall briefly the experimental method we have used. The vibrationally resolved cross sections are presented in section 3 and the assignments and decay paths of the Rydberg series are discussed in section 4.

2. Experimental

The experimental arrangement used in this work has been described in detail by Morin et al. [24]. We shall therefore give here only a brief summary of its main characteristics.

The synchrotron radiation produced by the ACO storage ring at Orsay (France) is monochromatized by a 1200 g/mm holographic grating and then crosses at right angle an effusive jet of gas. The pressure within the collision chamber is maintained between 5×10^{-5} and 10^{-4} Torr. The ejected photoelectrons are energy analysed by a 127° cylindrical analyser in a direction where the angular effects are minimized. This analyser is operated with a constant pass energy leading to a constant resolution of 70 meV. Taking into account the bandpass of the monochromator (0.2–0.25 nm), this resolution allows to separate the vibrational levels of the CO^+ X, A and B states.

The spectra are recorded in the CIS mode [22], i.e. keeping $h\nu-\epsilon_k$ constant to obtain directly the variation with energy of a given vibronic state cross section. These data are corrected for the variations of the incident photon flux and of the pressure and for the transmission of the analyser. The relative vibrationally resolved partial cross sections obtained in this way have been normalized using the data of Samson and Gardner [23,4] at a few wavelengths between 74.5 and 63.7 nm.

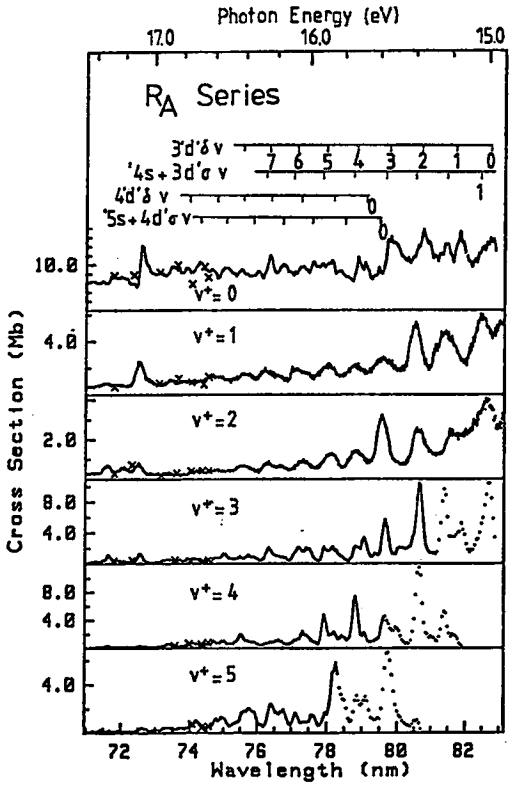

Fig. 1. Experimental vibrationally resolved cross sections for the production of CO^+ X $^2\Sigma^+$. We have represented by dotted lines the very low kinetic energy parts of these cross sections: in this region, the intensities are only qualitative since the correction for the transmission of the electron analyzer is not very accurate. The crosses correspond to the data of Samson and Gardner [23,4].

3. Vibrationally resolved photoionization cross sections

In fig. 1, we display the vibrationally resolved photoionization cross sections for the production of CO^+ X $^2\Sigma^+$ $v^+=0$ to 5 between 71 and 83 nm. The X $^2\Sigma^+$ $v^+=0$ to 3 cross sections at lower wavelength are presented in fig. 2, whereas fig. 3 shows the A $^2\Pi$ $v^+=0$ and 1 cross sections in the same region.

3.1. Production of CO^+ X $^2\Sigma^+$

The small difference of geometry between CO X $^1\Sigma^+$ and CO^+ X $^2\Sigma^+$ ($R_e=1.128$ and 1.115 Å respectively [19]) leads to a dominant production of CO^+ X $^2\Sigma^+$ $v^+=0$ by direct ionization. The decay of the R_B states populates CO^+ X $^2\Sigma^+$ vibrational levels up to $v^+=3$. At lower energy, the decay of the R_A states (mainly of the R_A-I series of Ogawa and Ogawa [15]) allows the production of higher vibrational levels (up to $v^+=9$ [4]). This behaviour is linked to the values of the internuclear distances of the CO^+ A $^2\Pi$ and B $^2\Sigma^+$ states, to which these series converge and which are 1.244 and 1.169 Å, respectively [19]. We observe in figs. 1 and 2 that the intensities of both R_A and R_B resonances vary strongly with the vibrational level of the ion. In the case of the Rydberg states associated with B $^2\Sigma^+$ we observe furthermore a strong variation of the shape of the

profiles as a function of the vibrational channel: the structures at 72.6, 68.1 and 65.7 nm display this behaviour. For these two latter resonances, the profile changes from a window shape ($v^+ = 0$) to a lorentzian shape ($v^+ \geq 1$). As a result, the vibrational branching ratios are strongly energy dependent, leading to variations of the vibrational structure of the electronic bands in the photoelectron spectra when the photon energy is modified. In particular, broad structures, probably resulting from the superposition of several resonances, appear at the wavelengths of the NeI resonance lines (74.4 and 73.6 nm). These structures are, however, weak, explaining why the transition to $X\ ^2\Sigma^+$ $v^+ = 0$ still represents 70% of the photoelectron band [3,4].

3.2. Production of $CO^+\ A\ ^2\Pi$

In the spectral range investigated here, the vibrationally resolved partial cross sections associated with the $A\ ^2\Pi$ ionic state (fig. 3) are most strongly perturbed by the R_B autoionizing series. In the two vibrational channels considered ($v^+ = 0$ and 1), the "sharp" and "diffuse" series are dominant. We must point out that, at the energy of the sharp $n = 3$ resonance, we measure an electronic branching ratio of about 0.4 for the $X\ ^2\Sigma^+$ channel in agreement with the PES results of Plummer et al. [22]. As in the $X\ ^2\Sigma^+$ cross sections, we observe important variations of the intensity ratios between the resonances as a function of the ion vibrational level.

Apart from these R_B resonances, one also observes a structure near 72.2 nm (17.2 eV) (fig. 3). This structure also appears in the $X\ ^2\Sigma^+$ cross sections (see fig. 2) and, as will be discussed in further detail below, results most probably from Rydberg series converging to vibrationally excited states of $CO^+\ A\ ^2\Pi$ [15,20].

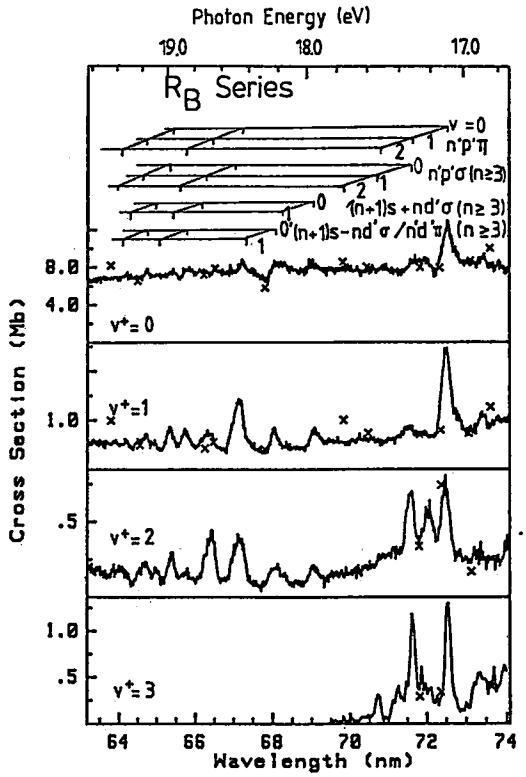

Fig. 2. Experimental vibrationally resolved cross sections of $CO^+\ X\ ^2\Sigma^+$ in the region of the R_B states. Crosses correspond to the data of Samson and Gardner [23,4].

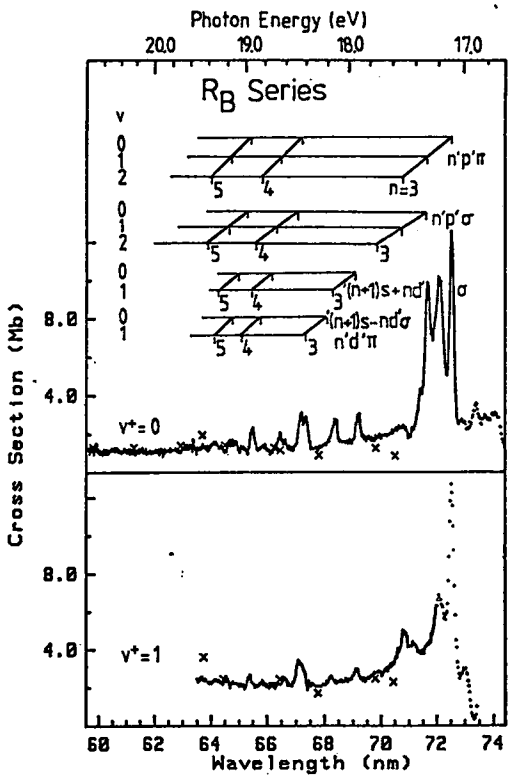

Fig. 3. Experimental vibrationally resolved cross sections for the production of $CO^+\ A\ ^2\Pi$. Crosses correspond to the data of Samson and Gardner. The cross sections at low kinetic energy, represented by dotted lines, are only qualitative.

4. Discussion

4.1. Rydberg series converging to $CO^+ A\,^2\Pi$

In order to clarify the assignments of the numerous structures appearing in the 78–83 nm region (17.0–14.9 eV), we have performed an ab initio calculation of the energies of the first members of the Rydberg series converging to $CO^+ A\,^2\Pi$ using a method developed by Lefebvre-Brion [25]. The basis set used is described in ref. [18]. The results are summarized in table 1, together with the transition moments and widths taken from our previous work [18]. These widths have been calculated from the bielectronic interactions using the Fermi golden rule. The data of table 1 show that three series are dominant: $A\,^2\Pi$ '$(n+1)$s + nd'σ, n'd'δ and n'd'π.

Further comparison with the experimental data requires the calculation of the total photoionization cross section (which coincides here with the $X\,^2\Sigma^+$ partial cross section as the $A\,^2\Pi$ channel is closed in this region) and of the $X\,^2\Sigma^+$ vibrationally resolved partial cross sections. For the calculation of the total cross section, we have used the Fano–Cooper [26,27] theory. The vibrationally resolved cross sections have been calculated within the Fano [26]–Starace [28]–Smith [29] formalism. The general characteristics of the present model are then [26,29]:

(i) The resonances are considered as isolated. No overlap between the resonances occurs. This is fully justified in the 77–84 nm region owing to the weak widths of the Rydberg states of Π total symmetry (see table 1).

(ii) The transition moments and bielectronic interactions are written as a product of an electronic and a vibrational factor (Condon approximation). This latter factor is the overlap integral between the vibrational functions of the two states involved. We recall (see section 1) that this level of approximation does not account for the pure vibrational autoionization.

The other characteristics of our model are specific to the particular problem discussed here:

(i) We have only taken into account the R_A 's + d'σ, 'd'δ and 'd'π series, thus neglecting the low-intensity series 'p'σ, 'p'π and 's − d'σ) (see table 1). The electronic transition moments and bielectronic interactions are taken from ref. [18].

(ii) for the calculation of the vibrational overlap integrals, we have assumed that the R_A states have all the same potential energy curve as $CO^+ A\,^2\Pi$. The nuclear wavefunctions of the CO $X\,^1\Sigma^+$

Table 1
Quantum defects, intensities and widths of the R_A series

R_A series	Quantum defect μ	Reduced intensity [a] I_r (au)	Reduced width [a] Γ_r (eV)
's+d'σ	1.164	2.349	0.189
's−d'σ	−0.090	0.080	0.099
'p'σ	0.59	0.017	0.155
'p'π	0.62	0.016	0.614
'd'π	0.16	11.960	2.579
'd'δ	0.03	2.861	0.034

[a] The intensities (I) and widths (Γ) are related to the corresponding reduced quantities (I_r and Γ_r) by the relations $I = I_r/(n-\mu)^3$ and $\Gamma = \Gamma_r/(n-\mu)^3$, where n is the principal quantum number and μ the quantum defect.

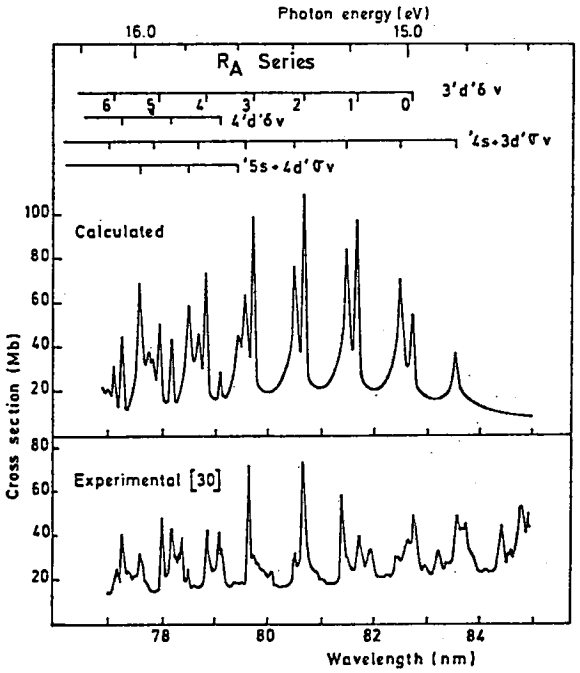

Fig. 4. Calculated total photoionization cross section in the region of the R_A series; these results have been broadened to a resolution of 0.007 nm. The experimental data are from Berkowitz [30].

$v = 0$, R_A v and CO^+ X $^2\Sigma^+$ v^+ states have been approximated by Morse functions.

The total photoionization spectrum presented in fig. 4 shows clearly that the observed resonances (series R_A-I of Ogawa and Ogawa [15], Henning's H(1) and H(2) progressions [11], Tanaka's P(1), P(2) and P(3) progressions [12]) can be assigned to the 's + d'σ and 'd'δ series, whereas 'd'π modulates the background.

In table 2, we compare the observed [13,15] and calculated wavelengths for these series and progressions.

Due to the great number of vibronic Rydberg states in this region and within our experimental resolution (0.2–0.25 nm), the structures observed in fig. 1 correspond to two or more states which are not necessarily characterized by the same vibrational quantum number v. To disentangle

Table 2
Experimental and calculated wavelengths (nm) of the Rydberg states converging to CO^+ A $^2\Pi$ [a]

Ogawa and Ogawa R_A-I series [15]

v	R_A-I $n = 3$ exp.	3'd'δ calc.	R_A-I $n = 4$ exp.	4'd'δ calc.	R_A-I $n = 5$ exp.	5'd'δ calc.
0	82.76	82.73	79.10	79.12	77.52	77.58
1	81.71	81.69	78.15	78.17	76.62	76.67
2	80.71	80.69	77.24	77.26	75.74	75.79
3	79.75	79.74	76.37	76.38	74.90	74.95
4	78.83	78.83	75.53	75.55	74.09	74.14
5	77.96	77.95	74.72	74.74	73.32	73.37
6	77.13	77.11	73.95	73.97	–	72.62
7	76.31	76.30	73.21	73.22	71.86	71.91
8	75.53	75.53	72.48	72.51	71.16	71.22

Henning's H(1) and H(2) progressions [11]

H(1)			H(2)		
exp. wavelength [13]	calc. wavelength	assignment	exp. wavelength [13]	calc. wavelength	assignment
83.86			83.62	83.56	'4s + 3d'σ $v = 0$
82.80	82.73	3'd'δ $v = 0$	82.45	82.50	'4s + 3d'σ $v = 1$
81.75	81.69	3'd'δ $v = 1$	81.44	81.49	'4s + 3d'σ $v = 2$
80.70	80.69	3'd'δ $v = 2$	80.50	80.51	'4s + 3d'σ $v = 3$
79.77	79.74	3'd'δ $v = 3$	79.67	79.58	'4s + 3d'σ $v = 4$

Tanaka's P(1), P(2) and P(3) progressions [12]

P(1)			P(2)			P(3)		
exp. [13]	calc.	assignment	exp. [13]	calc.	assignment	exp. [13]	calc.	assignment
79.12	79.12	4'd'δ $v = 0$	77.69	77.58	'5s + 4d'σ $v = 2$	77.54	77.58	5'd'δ $v = 0$
78.18	78.17	4'd'δ $v = 1$		77.58	5'd'δ $v = 0$		77.58	'5s + 4d'σ $v = 2$
77.26	77.26	4'd'δ $v = 2$		77.74	'6s + 5d'σ $v = 0$	76.69	76.67	5'd'δ $v = 1$
76.39	76.38	4'd'δ $v = 3$	76.77	76.77	6'd'δ $v = 0$		76.69	'5s + 4d'σ $v = 3$
75.54	75.55	4'd'δ $v = 4$	75.90	75.88	6'd'δ $v = 1$	75.81	75.79	5'd'δ $v = 2$
74.75	74.74	4'd'δ $v = 5$	75.03	75.02	6'd'δ $v = 2$		75.85	'5s + 4d'σ $v = 4$
						74.96	74.95	5'd'δ $v = 3$
73.97	73.97	4'd'δ $v = 6$	74.20	74.20	6'd'δ $v = 3$		75.03	'5s + 4d'σ $v = 5$
73.22	73.22	4'd'δ $v = 7$	73.35	73.40	6'd'δ $v = 4$	74.15	74.14	5'd'δ $v = 4$

[a] The calculated wavelengths are based on the data of table 1. For the vibrational spacings, we have assumed that the R_A states and CO^+ A $^2\Pi$ have the same potential energy curve with the following parameters: $\omega_e = 1562.06$ cm^{-1} and $\omega_e x_e = 13.53$ cm^{-1} [19].

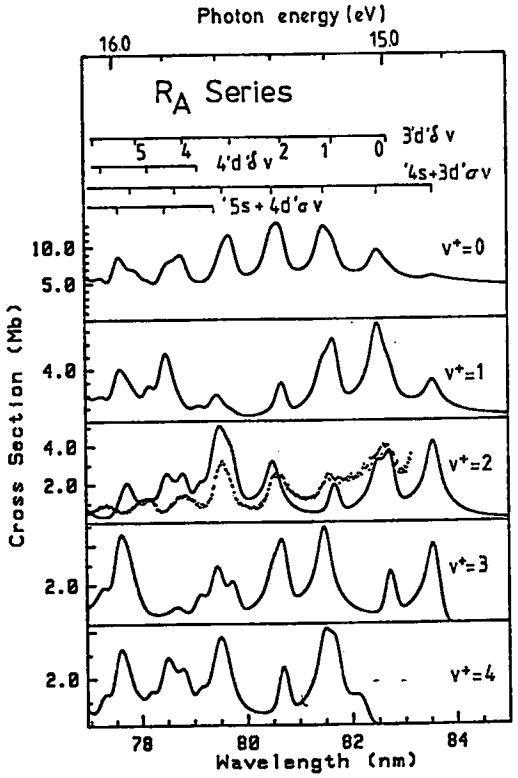

Fig. 5. Calculated vibrationally resolved cross sections for the production of CO^+ $X\ ^2\Sigma^+$ in the region of the R_A states. The spectra have been broadened to a resolution of 0.2 nm to correspond to the experimental data of fig. 1. As an example, the experimental $X\ ^2\Sigma^+$ $v^+ = 2$ cross section is represented by a dotted line.

this puzzle, we have calculated the vibrationally resolved cross sections: these results are displayed in fig. 5 and should be compared with the data of fig. 1.

We observe first of all that the enhancement of the $X\ ^2\Sigma^+$ $v^+ > 1$ cross sections with respect to the off-resonance situation is well accounted for by our calculations. Within our simple model, this behaviour must be correlated to the vibrational overlap integrals connecting the CO $X\ ^1\Sigma^+$ $v = 0$, the CO R_A v and the CO^+ $X\ ^2\Sigma^+$ v^+ states: the difference of geometry between the R_A and the CO^+ X states ($R_e = 1.115$ and 1.244 Å respectively [19]) is responsible for the non-negligible values of the $\langle v | v^+ \rangle$ overlaps when v^+ is greater than 1 and thus for the enhancement of the corresponding cross sections.

The comparison of figs. 1 and 5 reveals that the peaks observed at high wavelength ($\lambda > 79$ nm) result from the superposition of '$(4s + 3d)'\sigma$ $v + 1$ and $3'd'\delta$ v. The behaviour of these structures as a function of the ionic vibrational level is therefore not so simple as it would have been expected. For a number of these structures, the agreement between the experimental and calculated cross sections is satisfactory: the positions of the resonances are reproduced within a precision of about 0.1 nm (20 meV) and the relative intensities agree in many cases qualitatively.

Such a result is satisfactory if we consider that with our very simple model (see the approximations stated above), we did not attempt to give a quantitative description of the resonance but rather we tried to obtain a qualitative framework to interpret a complicated vibrational pattern.

As examples, we discuss now in further detail a few of the numerous structures appearing in this spectral range. The peak located near 82.6 nm corresponds to R_A $'4s + 3d'\sigma$ $v = 1$ and R_A $3'd'\delta$ $v = 0$. The position of its maximum in each vibrationally resolved cross section is respectively 82.70 ($v^+ = 0$), 82.50 ($v^+ = 1$), 82.70 ($v^+ = 2$) and 82.67 nm ($v^+ = 3$), whereas the calculated maxima are located at, respectively, 82.5, 82.5, 82.72 and 82.72 nm. As can be seen from the values of table 2, this means that $'4s + 3d'\sigma$ $v = 1$ dominates the $v^+ = 0$ and $v^+ = 1$ curves and that $3'd'\delta$ $v = 0$ dominates the $v^+ = 2$ and $v^+ = 3$ curves. This behaviour is linked to the fact that the $\langle CO^+ X\ ^2\Sigma^+ v^+ \leqslant 1 | R_A\ v = 1 \rangle$ overlaps are larger than the $\langle CO^+ X\ ^2\Sigma^+ v^+ \leqslant 1 | R_A\ v = 0 \rangle$ ones: this inequality is inverted for $v^+ \geqslant 2$. The experimental intensities – 15.8, 5.9, 4 and 10.4 Mb for $v^+ = 0$, 1, 2 and 3, respectively – are in qualitative agreement with the calculated values (10.0, 8.2, 4.2 and 3.2 Mb).

Another structure, located around 80.6 nm, results from the superposition of $'4s + 3d'\sigma$ $v = 3$ and $3'd'\delta$ $v = 2$. The experimental positions and intensities in the $v^+ = 0$ to 4 channels are 80.74 nm ($\sigma = 17.7$ Mb), 80.53 nm ($\sigma = 5.3$ Mb), 80.57 nm ($\sigma = 2.6$ Mb), 80.64 nm ($\sigma = 10.4$ Mb) and 80.64 nm ($\sigma = 11.5$ Mb). The corresponding

calculated values are 80.68 nm ($\sigma = 13.6$ Mb), 80.7 nm ($\sigma = 3.2$ Mb), 80.5 nm ($\sigma = 3.4$ Mb), 80.68 nm ($\sigma = 4.7$ Mb) and 80.7 nm ($\sigma = 2.9$ Mb). For these two typical examples, we observe a qualitative agreement for the positions and intensities of the resonances: the Condon approximation is thus very useful for a qualitative understanding of their decay. Nevertheless, as the observed peaks in the convoluted spectra are made up of two (or more) resonances, their intensities and positions result from a complicated balance between the electronic (transition moments snf bielectronic interactions) and the vibrational (overlap integrals) quantities. The divergences between the calculated and experimental cross sections can then be due to the electronic data which have been obtained by ab initio calculations (from ref. [18]).

In this discussion, we have not considered the possibility of complex resonances [31,20] related to the opening of the $X\ ^2\Sigma^+\ v^+ = 4$, 5 and 6 channels between 83.7 and 79.5 nm. This effect is, however, expected to be small in the present case.

4.2. Rydberg series converging to $CO^+ B\ ^2\Sigma^+$

In figs. 2 and 3, we have reported the assignments of the Rydberg series as deduced from the theoretical work of Leyh and Raseev [18] who have calculated the total, partial ($CO^+ X\ ^2\Sigma^+$ and $A\ ^2\Pi$) and vibrationally resolved ($X\ ^2\Sigma^+\ v^+ = 0$ to 3) photoionization cross sections of CO in the R_B region by a variant of the two-step MQDT. We must emphasize that this method is very sophisticated compared to the simple model retained in the present paper for the R_A series. In particular, MQDT is not restricted to isolated resonances but allows to treat the whole of a Rydberg series.

We shall not discuss further here the vibrationally resolved cross sections of the $X\ ^2\Sigma^+$ state: a detailed discussion is given in ref. [18]. The main conclusion is that the Condon approximation provides a satisfactory framework for the interpretation of the vibrational behaviour of the R_B resonances.

We now consider the $A\ ^2\Pi\ v^+ = 0$ and 1 cross sections. For these two exit channels, the $R_B\ v = 0$ resonances dominate. In the $A\ ^2\Pi\ v^+ = 0$ channel, however, the $R_B\ v = 1$ states have a mean intensity twice as weak as that of the $R_B\ v = 0$ states, whereas the $R_B\ v = 2$ states have an extremely low intensity. The opposite occurs in the $A\ ^2\Pi\ v^+ = 1$ channel: in this case, the $R_B\ v = 1$ states are very weak but the contribution of the $R_B\ v = 2$ resonances is no more negligible.

We can, in a first approach, neglect the contribution of the direct $CO\ X\ ^1\Sigma^+\ v = 0 \rightarrow CO^+\ A\ ^2\Pi\ v^+ = 0, 1 + e^-$ process. In this case, the resonances have a lorentzian shape. Smith [29] has shown that, within the Condon approximation, the vibrational branching ratios for the decay of an isolated lorentzian resonance are simply given by the square of the vibrational overlaps between the Rydberg and the ionic states. The overlap between the ground neutral state and the Rydberg state must not be considered as it remains constant for the decay of a given resonance. With notations adapted to the present problem the branching ratios can then be written:

$$\left|\left\langle CO\ R_B\ v \middle| CO^+\ A\ ^2\Pi\ v^+\right\rangle\right|^2$$

For a $R_B\ v = 0$ state, we obtain the following branching ratios: 0.415 for the $A\ ^2\Pi\ v^+ = 0$ channel and 0.315 for the $v^+ = 1$ channel. The branching ratios for a $R_B\ v = 1$ state are 0.433 ($v^+ = 0$) and 0.012 ($v^+ = 1$) whereas for a $R_B\ v = 2$ resonance we calculate the following values: 0.139 ($v^+ = 0$) and 0.381 ($v^+ = 1$). These values reproduce well the observed situation: the $R_B\ v = 1$ states decay mainly in the $A\ ^2\Pi\ v^+ = 0$ channel but the decay of the $R_B\ v = 2$ resonances leads preferentially to $A\ ^2\Pi\ v^+ = 1$. In this case also, the Condon factorization allows to understand qualitatively the experimental results. Let us, however, note that the presence of a background (direct ionization) which represents, at the position of $R_B\ 3'p'\pi\ v = 0$, 20% of the $A\ ^2\Pi$ partial cross section indicates that these resonances cannot be exactly lorentzian.

The main structures between 64 and 74 nm can be assigned to the R_B states except for the peak observed at 72.2 nm between the first members of the R_B sharp and diffuse series. Ogawa and Ogawa [15] have assigned this structure to the $n = 9$, 10, 11 Rydberg states converging to $CO^+\ A\ ^2\Pi\ v = 4$. The decay of these resonances in the vibrational

channels of $CO^+ X\ ^2\Sigma^+$ must then be governed by the

$$\left|\left\langle CO\ R_A\ v=4 \middle| CO^+ X\ ^2\Sigma^+\ v^+\right\rangle\right|^2$$

matrix element which has negligible values for odd v^+. This corresponds exactly to the v^+ dependence of the 72.2 nm structure (fig. 2) confirming the interpretation of Ogawa and Ogawa [15]. In the $A\ ^2\Pi$ cross sections (fig. 3), we observe the appearance of this structure in the $v^+=0$ and $v^+=1$ channels.

This violates Berry's propensity rule [32] ($\Delta v=-1$) for vibrational autoionization which states that resonances associated with a $A\ ^2\Pi$ $v=4$ ionic core should mainly decay in the $A\ ^2\Pi$ $v=3$ channel. In their $A\ ^2\Pi$–$X\ ^2\Sigma^+$ FES experiments, Ito et al. [21] also observed vibrational autoionization structures with Δv values up to -5. This suggests a more subtle mechanism involving a coupling between the electronic and vibrational autoionizations. Other examples of such a behaviour have been evidenced in H_2 [33,34], NO [35,36] and PF_3 [37].

5. Conclusions

In this paper, we have reported new continuous measurements of the vibrationally resolved cross sections of $CO^+ X\ ^2\Sigma^+$ and $A\ ^2\Pi$ in the region of the Rydberg states converging to $CO^+ A\ ^2\Pi$ and $B\ ^2\Sigma^+$. The electronic autoionization of these Rydberg series produces strong variations of the vibrational branching ratios with the photon energy: the amount of vibrational excitation in the photoelectron spectrum depends therefore strongly on the excitation energy.

We have suggested new unambiguous assignments of the main observed progressions and series appearing between 73 and 83 nm and converging to $CO^+ A\ ^2\Pi$. The R_A 's + d'σ, 'd'δ and 'd'π resonances dominate the photoionization spectrum in this spectral range. We have interpreted the decay of these R_A resonances in the $CO^+ X\ ^2\Sigma^+$ v^+ channels using a simple model, based on the Condon approximation and ab initio data from a previous work [18]. We have also shown that the interpretation of Ogawa and Ogawa [15] for the broad structure located near 72.2 nm (17.2 eV) agrees with our vibrationally resolved results for the $X\ ^2\Sigma^+$ state. In the $A\ ^2\Pi$ v^+ channels, we observe that the decay of the resonances giving rise to that structure violates Berry's propensity rule [32].

The results presented in this paper and in ref. [18] show that the Condon approximation allows a qualitative understanding of the vibrational selectivity of the electronic autoionization. For a quantitative agreement to be obtained, at least three conditions should be fulfilled. We should first of all have very precise electronic quantities which are not yet available to us. Secondly, the variation with R of these quantities should be taken into account: whether this will have important consequences is however difficult to evaluate.

The third requirement is most probably of great importance in the present case. Above 70 nm, the ionization yield of CO is known to be lower than unity [23]. At 74.51 nm, this yield is equal to 0.66. This behaviour is due to the presence of a few dissociation asymptotes in this energy range leading to a competition between ionization and dissociation into neutral fragments [38,39]. It would then be necessary to take into account the different couplings between the Rydberg series, the ionization continua and the dissociation continua. These couplings can deeply perturb the vibrational excitation of the $CO^+ A\ ^2\Pi$ and $X\ ^2\Sigma^+$ states.

Our work confirms the results of Plummer et al. [22] and of Ederer et al. [5] on the A/X branching ratio at the energy of the R_B sharp $n=3$ resonance. No definite explanation has unfortunately been found for the disagreement with the FES results of Ito et al. [21].

The most intense series converging to $CO^+ B\ ^2\Sigma^+$ are associated with Rydberg orbitals of 'p' character [18] (see figs. 2 and 3); in the R_A case however, the most intense series have a 's' or 'd' character. In the N_2 isoelectronic system, among the Rydberg series converging to $N_2^+ A\ ^2\Pi_u$ and $B\ ^2\Sigma_u^+$, only those having a 's' or 'd' character (g symmetry) can be reached by a dipolar transition. This N_2/CO comparison leads to the conclusion that the $CO^+ B\ ^2\Sigma^+$ ionic core is much more

heteronuclear than the CO^+ $A\,^2\Pi$ one. This conclusion is supported by the value of the CO^+ dipole moment which is larger for the B state than for the A state: at the center of mass, the dipole moment of CO^+ $B\,^2\Sigma^+$ and $A\,^2\Pi$ are respectively 0.80 and 0.27 au.

Acknowledgement

We are grateful to our colleagues P. Morin, M.Y. Adam and P. Lablanquie for their major contributions for the setting-up of the experiment and for helpful discussions. We also thank P. Roy for her help in the measurements. The technical staff of LURE is acknowledged for operating the storage ring and for general facilities. We are grateful to G. Raşeev for many fruitful discussions and for having suggested several important improvements in the manuscript. The Fonds National de la Recherche Scientifique of Belgium and the NATO (contract no. 096.82) are acknowledged for their financial contribution.

References

[1] J.L. Dehmer, D. Dill and A.C. Parr, in: Nato ASI series C142, Photophysics and photochemistry in the vacuum ultraviolet, eds. S. Mc. Glynn, G. Findley and R. Huebner (Reidel, Dordrecht, 1985).
[2] V. Mc. Koy, T.A. Carlson and R.R. Lucchese, J. Phys. Chem. 88 (1984) 3188.
[3] P. Natalis, J. Delwiche and J.E. Collin, Chem. Phys. Letters 13 (1972) 491.
[4] J.L. Gardner and J.A.R. Samson, J. Electron Spectry. 13 (1978) 7.
[5] D.L. Ederer, A.C. Parr, B.E. Cole, R. Stockbauer, J.L. Dehmer, J.B. West and K. Codling, Proc. Roy. Soc. A 378 (1981) 423.
[6] P. Natalis, J. Delwiche, J.E. Collin, G. Caprace and M. Th. Praet, Chem. Phys. Letters 49 (1977) 177.
[7] P. Morin, I. Nenner, M.Y. Adam, M.-J. Hubin-Franskin, J. Delwiche, H. Lefebvre-Brion and A. Giusti-Suzor. Chem. Phys. Letters 92 (1982) 609.
[8] P. Natalis, Mémoires de l'Académie Royale de Belgique, Classe des Sciences, 2ème série, XLI fasc. 1 (1973).
[9] A.W. Potts and G.H. Fattahallah. J. Phys. B 13 (1980) 2545.
[10] M.-J. Hubin-Franskin, J. Delwiche, P. Morin, M.Y. Adam, I. Nenner and P. Roy, J. Chem. Phys. 81 (1984) 4246.
[11] A.J. Henning. Ann. Physik 13 (1932) 599.
[12] Y. Tanaka, Sci. Papers Inst. Chem. Res. (Tokyo) 39 (1942) 447.
[13] R.E. Huffman, J.C. Larrabee and Y. Tanaka, J. Chem. Phys. 40 (1964) 2261.
[14] M. Ogawa, J. Chem. Phys. 43 (1965) 2142.
[15] M. Ogawa and S. Ogawa, J. Mol. Spectry. 41 (1972) 393.
[16] J.H. Fock, P. Gürtler and E.E. Koch, Chem. Phys. 47 (1980) 87.
[17] E. Lindholm, Arkiv Fysik 40 (1969) 103.
[18] B. Leyh and G. Raşeev, Phys. Rev. A 34 (1986) 2920.
[19] K.P. Huber and G. Herzberg, Molecular spectra and molecular structure, Vol. 4. Constants of diatomic molecules (Van Nostrand–Reinhold, New York, 1979) p. 166.
[20] G. Raşeev, B. Leyh and H. Lefebvre-Brion, Z. Physik D 2 (1986) 319.
[21] K. Ito, A. Tabché-Fouhailé, H. Fröhlich, P.M. Guyon and I. Nenner, J. Chem. Phys. 82 (1985) 1231.
[22] E.W. Plummer, T. Gustafsson, W. Gudat and D.E. Eastman, Phys. Rev. A 15 (1977) 2339.
[23] J.A.R. Samson and J.L. Gardner, J. Electron Spectry. 8 (1976) 35.
[24] P. Morin, M.Y. Adam, I. Nenner, J. Delwiche, M.-J. Hubin-Franskin and P. Lablanquie, Nucl. Instr. Methods 208 (1983) 761.
[25] H. Lefebvre-Brion, J. Mol. Spectry. 19 (1973) 103.
[26] U. Fano, Phys. Rev. 124 (1961) 1866.
[27] U. Fano and J.W. Cooper, Phys. Rev. 137 (1965) A1364.
[28] A.F. Starace, Phys. Rev. A 16 (1977) 231.
[29] A.L. Smith, Phil. Trans. Roy. Soc. London A 268 (1970) 169.
[30] J. Berkowitz, in: Photoabsorption, photoionization and photoelectron spectroscopy (Academic Press, New York, 1979) p. 228.
[31] A. Giusti-Suzor and H. Lefebvre-Brion, Phys. Rev. A 30 (1984) 3057.
[32] R.S. Berry, J. Chem. Phys. 45 (1966) 1228.
[33] J. Berkowitz and W.A. Chupka, J. Chem. Phys. 51 (1969) 2341.
[34] M. Raoult and Ch. Jungen, J. Chem. Phys. 74 (1981) 3388.
[35] Y. Ono, S.H. Linn, H.F. Prest, C.Y. Ng and E. Miescher, J. Chem. Phys. 73 (1980) 4855.
[36] A. Giusti-Suzor and Ch. Jungen, J. Chem. Phys. 80 (1984) 986.
[37] J. Berkowitz and J.P. Greene, J. Chem. Phys. 81 (1984) 4328.
[38] J.H.D. Eland, J. Chim. Phys. 77 (1980) 613.
[39] A. Tabché-Fouchailé, M.J. Hubin-Franskin, J.P. Delwiche, H. Fröhlich, K. Ito, P.M. Guyon and I. Nenner, J. Chem. Phys. 79 (1983) 5894.